

DEVELOPMENT OF FPGA-BASED TDC WITH WIDE DYNAMIC RANGE FOR MONITORING THE TRIGGER TIMING DISTRIBUTION SYSTEM AT THE KEKB INJECTOR LINAC

Tsuyoshi Suwada*, Kazuro Furukawa, Fusashi Miyahara, KEK, Tsukuba, Japan

Abstract

A new field-programmable gate array (FPGA)-based time-to-digital converter (TDC) with a wide dynamic range greater than 20 ms has been developed to monitor the timing of various pulsed devices in the trigger timing distribution system of the KEKB injector linac. The pulsed devices are driven by feeding regular as well as any irregular (or event-based) timing pulses. For monitoring the timing as precisely as possible, a 16-ch FPGA-based TDC has been developed on a Xilinx Spartan-6 FPGA equipped on VME board with a time resolution of 1 ns. The resolution was achieved by applying a multisampling technique, and the accuracies were 2.6 ns (rms) and less than 1 ns (rms) within the dynamic ranges of 20 ms and 7.5 ms, respectively. The various nonlinear effects were improved by implementing a high-precision external clock with a built-in temperature-compensated crystal oscillator.

INTRODUCTION

Recent advances in FPGA technology have made it possible to apply them to TDCs in which the FPGA is embedded (called FPGA-based TDCs) in high-energy particle and nuclear physics [1] and also in materials science [2]. FPGA-based TDCs are very attractive because of their high performance, high-speed data transfer, and customizability and flexibility in precision timing measurements without any external complex hardware. These excellent features enable high-precision time-duration measurements down to a few picoseconds (see references in [1]). These features also enable the possibility of new applications to precisely monitor various timing pulses with a wide dynamic range in large accelerator complexes, where an accuracy of a few nanoseconds is sufficient.

We have developed a new FPGA-based TDC required for application to the KEKB injector linac. The required specifications of the TDCs are a wide dynamic range greater than 20 ms and an accuracy of 1 nanosecond level, where low-cost fabrication should be also required. The basic design, development, and experimental results of the new FPGA-based TDC for applications to large accelerator complexes are reported in detail.

FPGA-BASED TDC

Required Specifications

All downstream storage rings of the KEKB injector linac [3] will be filled in top-up injections based on a pulse-

by-pulse modulation scheme at 50 Hz, which allows the injector linac to perform virtually simultaneous injections [4]. For the virtually simultaneous injections, a new trigger timing distribution system is under development on the basis of the event-based timing and control system [5]. A new additional system is also under development for monitoring all timing pulses generated in the trigger timing distribution system as precisely as possible [6]. The purpose of the introduction of a timing monitoring system is to increase the reliability of the event-based timing and control system. Because the injection beam charges need to be increased to be four to five times greater than those of the previous KEKB, such a timing monitoring system may serve not only the stable operation and complex simultaneous injection but also reliable radiation safety and machine protection of the injector linac.

The fiducial repetition frequency of the injector linac is based on 50 Hz. All pulsed devices are driven by the trigger timing pulses appropriately delayed from the fiducial timing. These trigger timing pulses are fundamentally generated with a frequency of 50 Hz at maximum by obeying the beam injection timing sequences programmed in the control system. However, in a strict sense, the fiducial time duration does not need to be determined exactly to be 20 ms owing to the synchronization condition of the linac and ring RF frequencies on the injection bucket position in the ring.

The allowable width of the fiducial time duration is restricted to the trigger timing condition for the modulators of the high-power klystrons in the injector linac because the modulators should be driven within 20 ± 1 ms to stabilize the applied voltage and to sufficiently allow for stable charging. This specification means that the allowable time duration of the fiducial timing should be monitored to maintain them within 20 ± 1 ms.

The trigger timing for most of other pulsed devices is less than 1 ms delayed from the fiducial timing, and more especially, the trigger timing for the beam-position monitors should be maintained at an accuracy of 1-ns level. Therefore, a resolution of 1 ns and a dynamic range greater than 20 ms are required for the time-duration measurements in the TDC along with a higher accuracy.

Basic Design

The present event-based trigger timing distribution system was constructed in a VME-based system, and accordingly, it was necessary to construct new TDCs (6U VME64x module) in the same VME-based system. The basic specifications required for the VME/FPGA-based TDC are listed in Table 1.

* tsuyoshi.suwada@kek.jp

Table 1: Basic Specifications Designed for the VME/FPGA-based TDC

Basic parameter	Value	Units
Number of common starts	1	
Number of stops	16	
Number of multistops	4	
Number of bits	32	
Dynamic range (max.)	4.3	s
Resolution	1	ns
Clock frequency	250	MHz
Gigabit Ethernet	available	

The TDC has a common start and sixteen stop input channels. The input voltage level is based on a Nuclear Instrumentation Module (NIM) standard with a 50-Ω input impedance. The fiducial pulse is fed into the common start input channel, and the delayed trigger pulses to the pulsed devices are fed into the stop input channels. Each delay time from the fiducial pulse and the time duration between the fiducial pulses are synchronously measured with 32-bit counters with a resolution of 1 ns. A wide dynamic range of 4.3 s can be implemented at maximum on a Xilinx Spartan-6 (XC6SLX75) FPGA [7]. A multistop function in each stop input channel is available by which the delay timings of successive trigger pulses (up to four at maximum) during one fiducial period generated on one trigger line can be synchronously measured. This is an important specification required for two-bunch acceleration in an RF pulse delivered from the A1 electron gun, in which the time duration between two bunches is exactly 96.3 ns [5]. The content of the buffer data in the FPGA can be accessed via an A32/D32 VME64x interface. The developed TDC module is shown in Fig. 1.

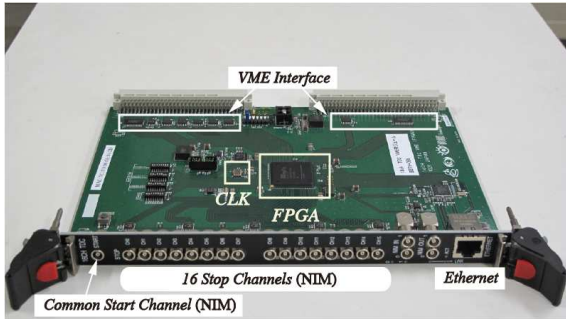


Figure 1: Developed VME/FPGA-based TDC module.

Basic Principle for the Time-duration Measurement

A fundamental principle of the TDC implementation is to count the number of the reference clock pulses generated during the time duration (T) between the leading edges of the start and stop pulses with a coarse counter, as shown in Fig. 2.

In such implementation schemes, the time resolution of the TDC is limited to T_{clk} at maximum, where T_{clk} is the time duration for a period of the reference clock when the

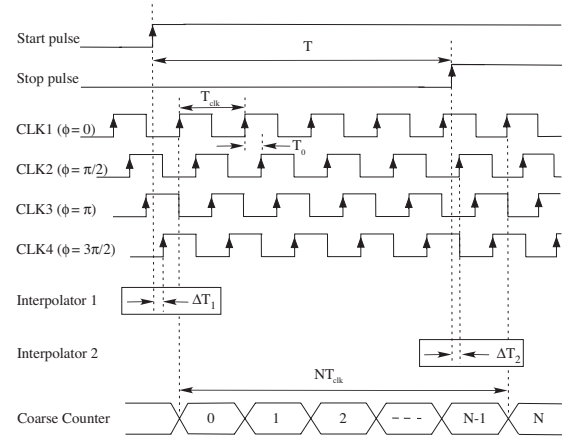


Figure 2: Timing diagram of the fundamental time-duration measurement of the TDC based on the multisampling technique.

start and stop pulses generated in the trigger timing distribution system are not synchronized at all with the reference clock of the TDC. There are several smart methods (sometimes called interpolation methods [8]) to improve the time resolution.

The time duration to be measured may be expressed as

$$T = NT_{clk} + (\Delta T_1 + \Delta T_{\phi 1}) - (\Delta T_2 + \Delta T_{\phi 2}), \quad (1)$$

where ΔT_1 (ΔT_2) is the fractional time duration measured between the leading edge of the start (stop) pulse and that of the next nearest pulse of the valid reference clock (CLK4 (CLK2) in this case), and $\Delta T_{\phi 1}$ ($\Delta T_{\phi 2}$) is the phase delay time of the valid reference clock with respect to the main reference clock (CLK1) ($\Delta T_{\phi 1} = T_{clk}/4$ ($\Delta T_{\phi 2} = 3T_{clk}/4$) in this case), although most of the time duration may be measured as NT_{clk} synchronously with the main reference clock (see Fig. 2). If the fractional time durations can be measured with a higher resolution on the basis of any interpolation method, the time resolution of the TDC may be comprehensively improved.

The multisampling (sometimes called 4×oversampling) technique [1] is one of many smart interpolation methods. In the multisampling technique, four similar reference clocks are generated in the FPGA with a period of T_{clk} , for which each relative phase difference is $\pi/2$, which corresponds to a delay time of $T_{clk}/4$, shown as CLK1–CLK4 (see Fig. 2). The fractional time, ΔT_1 (ΔT_2), for the start (stop) pulse can be measured by detecting the leading edge of the temporally closest reference clock by a first (second) interpolator with a four-times improved resolution of $T_0 = T_{clk}/4$, whereas most of the time duration (NT_{clk}) can be measured with a coarse counter driven by the main reference clock. The total time duration can be simply calculated based on eq. (1) by decoding and adding these results with a resolution of T_0 .

Circuit Architecture

Here, the generation of the reference clocks along with their relationships used in the TDC is described in detail. A

schematic block diagram of the circuit architecture of the TDC along with a block diagram of the phase-locked loop (PLL) are shown in Fig. 3.

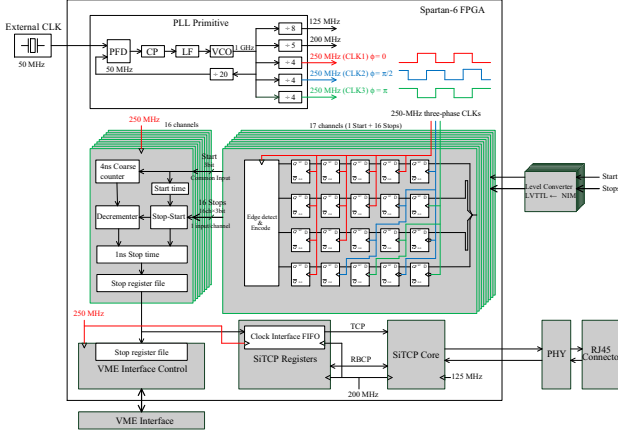


Figure 3: Schematic block diagram of the circuit architecture of the developed TDC. The meanings of the labels are detailed in text.

Three reference clocks, CLK1, CLK2 (delayed by $T_{clk}/4$), and CLK3 (delayed by $T_{clk}/2$), with each clock frequency of 250 MHz ($T_{clk} = 4$ ns) and a phase difference of $\pi/2$ are generated via a voltage-controlled oscillator (VCO) with a frequency of 1 GHz in the PLL primitive, where the frequency of the reference clock is divided by four through a frequency demultiplier. Two other frequencies, 200 MHz and 125 MHz, for the SiTCP and a physical layer transmitter and receiver of Ethernet (PHY) are generated by frequency-demultiplying the VCO frequency by five and eight, respectively. A frequency of 50 MHz is generated by frequency-demultiplying the VCO frequency by twenty, and it is directly phase-locked with the external clock via a standard digital PLL with a bandwidth of 4 MHz, which comprises a phase frequency detector (PFD), a charge pump (CP), and a loop filter (LF). Here, it is important to choose an external clock from a viewpoint of frequency stability because it dominantly influences the characteristics and performance of the TDC in terms of the frequency stability, jitter, skew, and temperature effects. An external 50-MHz temperature compensated crystal oscillator (TCXO, EPSON TG-5501CA [9]) has been selected during TDC development because its frequency stability is guaranteed within ± 1 ppm in a temperature (T_e) range of -40 to 85°C , for which the frequency stability is substantially an order smaller than that of standard crystal oscillators. The basic specifications of the external clock are listed in Table 2.

Table 2: Specifications of the External Clock

Parameter	Value	T_e Range
Frequency	50 MHz	
Stability	$< \pm 1.0 \times 10^{-6}$	$25 \pm 2^\circ\text{C}$
Property	$< \pm 0.28 \times 10^{-6} \text{ }^\circ\text{C}^{-1}$	-40 to 85°C

The fractional time durations (ΔT_1 and ΔT_2) are measured in the 1-ns interpolator as shown in Fig. 3. In the 1-ns interpolator, the start and stop pulses of the input signal are basically sampled and latched at respective D input via a flip-flop array with the use of both the leading and trailing edges of the two reference clocks with a phase difference of $\pi/2$ (CLK2 and CLK3, called sampling clocks), while another reference clock (CLK1, called system clock) is used as a sampling clock for the 4-ns coarse counter, and however, it works as the system clock in the 1-ns interpolator. In such a sampling scheme, the fractional time durations are determined by data sampled at the first row (4 flip-flops) of the flip-flop array. Thus, this sampling scheme is equivalent to that with the use of four different reference clocks with a phase difference of $\pi/2$ as shown in Fig. 2. It should be noted, however, that the system clock (CLK1) is not used at all for determining the fractional time durations in the 1-ns interpolator, while it is used only for determining the coarse time duration (NT_{clk}). This scheme is of advantage to save clock resources in the FPGA as much as possible and it is also due to increase the stability and reliability of the sampling clocks as much as possible by separating them from the system clock. A subsequent 4×4 flip-flop array is required for the two sampling clocks to be synchronized with the system clock domain and also to avoid any metastable states. Thus, the input signal is sampled five times each clock period in total.

In the decision logic (shown as “Edge detect & Encode”), the timing measurement result is converted to a 2-bit information along with an additional bit, which is used for an acknowledgement of both the valid edge detection and the valid phase with respect to the system clock. Then, a 3-bit and sixteen 3-bit information for the start and sixteen stop pulses, respectively, are sent to another logic where the measurement results are decoded. The fractional time duration measured in the 1-ns interpolator is decoded with its sign in a register (shown as “Stop-Start”). On the other hand, the coarse time duration is decoded in the 4-ns coarse counter. Both the coarse time and fractional time durations are simply calculated in a register (shown as “Decrementer”) with taking into account the signs of the fractional time durations based on eq. (1). The final result is stored in a register (shown as “1-ns Stop time”). Finally, the same data are moved to another register (shown as “Stop register file”) that can be accessed via a VME interface. It should be mentioned that in this decoding scheme the fiducial duration itself can be easily measured on the basis of the nominal start-stop implementation scheme even without any additional stop pulse, in which the next nearest start pulse is applied to the stop pulse.

EXPERIMENTAL TESTS

Characteristic Nonlinearity Measurements

The characteristic nonlinearity measurements were carried out with a high-precision rubidium time-based delay generator (SRS, Model DG645) for investigating these

systematic-error factors. Because the timing jitter of this delay generator is 10 ps/s (rms), the measurement errors expected from the delay generator are negligibly small. The start and stop pulses were generated with the delay generator, and they were fed into the TDC in an atmospheric environment. The time duration between the leading edges of the start and stop pulses was measured by changing the delay time to be set, where for simplicity, the asynchronous measurements were performed using the delay generator to drive the TDC. The results are shown in Fig. 4.

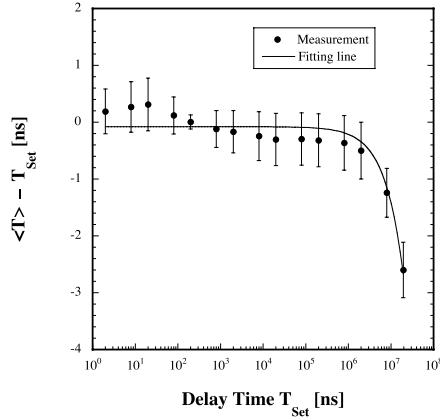


Figure 4: Variations in the time difference between the measured and set delay time with a dynamic range of 20 ms. Each solid point represents the average value over 5000 measurements and only the statistical error bars are plotted. The solid lines show a guide for the eyes only in a straight-line fitting.

Figure 4 shows the variations in the time difference between the measured and set delay time with a dynamic range of 20 ms, which is the required dynamic range. The non-linear point of the time difference curve is expected to be ~ 3 ms as shown in Fig. 4, and the absolute time difference at 20 ms is 2.6 ns. An 1-ns accuracy is attainable within the region less than 7.5 ms, and the quantization errors are dominant in this region.

The accuracy is generally given by the absolute time difference divided by the set delay time. The results are shown in Fig. 5 and show that the accuracy reaches a saturation point at which the set delay time is $T_{\text{set}} \sim 3$ ms, where the attained accuracy is 0.13 ppm, which may originate from the frequency stability of the external clock.

Precision and Integral Nonlinearity

The precision of the TDC is generally defined by a standard deviation of repetitive measurements of the time duration in which the quantization errors are dominant [10] if the systematic nonlinearity is sufficiently smaller within a given dynamic range; that is, the measurement errors are dominated by statistical errors. If in such measurement conditions the decimal part (c) of the ratio (T/T_0) is given by

$$c = \text{Frc}[T/T_0], \quad (2)$$

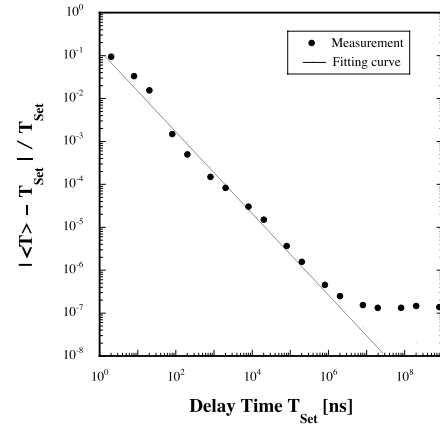


Figure 5: Variations in the accuracy as a function of the set delay time. The solid line is an exponential function fitted to the data.

the measurement precision (σ_T) is expressed by the following equation [8]:

$$\sigma_T = T_0 \sqrt{c(1-c)}. \quad (3)$$

The obtained precisions depending on the set delay time are shown in Fig. 6(a).

Here, the solid line shows calculations based on eq. (3), where the average values are applied to the parameter (T). The variations in the precision measurement are in good agreement with calculations. The obtained result means that the precision is mainly caused by the quantization errors within a dynamic range of 20 ms. The maximum (minimum) differential is 0.52 (0.13) ns. This result means that the least significant bit (LSB) due to quantization errors corresponds to 0.52 bits at maximum. The variations in the differential time difference between the measured and set delay time with a straight-line fitting within the same dynamic range are shown in Fig. 6(b).

The integral nonlinearity is defined by the maximum difference within a given dynamic range. The maximum integral nonlinearity is 0.39 ns at the set delay time of 20 ns. This result means $\text{LSB} = 0.39$ bits. Thus, the precision in the time-duration measurement may be expected to be less than 1 ns in total within a dynamic range of 20 ms. The obtained result is sufficiently acceptable for the trigger timing distribution system.

Temperature Stability

The temperature stability of the TDC was measured within a temperature region of $5\text{--}35^\circ\text{C}$ by changing the environmental temperature, where the TDC along with a VME crate without any CPUs were placed in a thermoregulated bath while the delay generator was outside. The results are shown in Fig. 7.

Figure 7(a) shows the variations in the difference ($\Delta\langle T \rangle$) between the measured time duration and the set delay time as a function of temperature, and Fig. 7(b) shows the differential coefficient with temperature as a function of the set delay

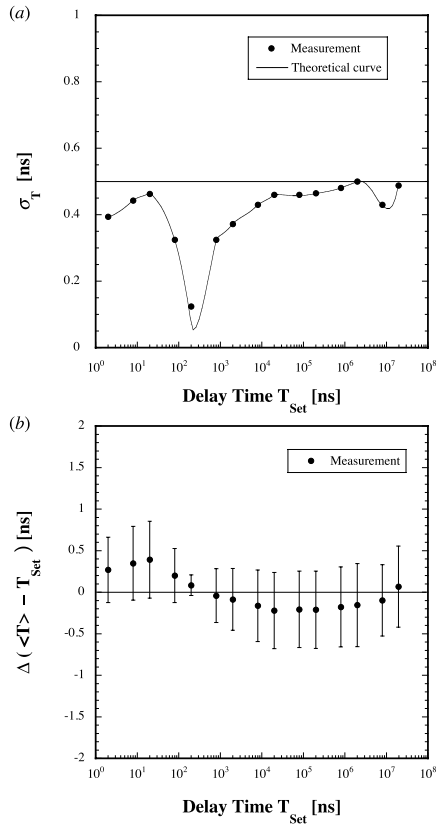


Figure 6: Variations (a) in the precision measurement depending on the set delay time within a dynamic range of 20 ms and (b) in the differential time difference between the measured and set delay time from a straight-line fitting within the same dynamic range.

time. In Fig. 7(a), it should be mentioned that the data points are shown as the differentials from the reference data measured at 25°C (room temperature).

The variations in the temperature stability cannot be expressed by any simple monotonic functions because the temperature effect is automatically compensated by feedback controls embedded in the external clock, and their characteristic feedback patterns may originate from its intrinsic temperature compensation scheme. The maximum measured time duration is $|\Delta\langle T \rangle| \sim 1$ ns at 20°C and a set delay time of 19.5 ms. The variations in the differential coefficient (C_T [ns/°C]) with temperature at 25°C are shown in Fig. 7(b). The magnitude of the coefficient starts to slightly increase at a set delay time greater than 2 ms. The obtained result is sufficiently acceptable for the trigger timing distribution system.

CONCLUSIONS

We have successfully fabricated and tested a new VME/FPGA-based TDC with a wide dynamic range greater than 20 ms and a resolution of 1 ns. The required specifications of the TDC were realized on the basis of the suitable design with a high-precision temperature-compensated ex-

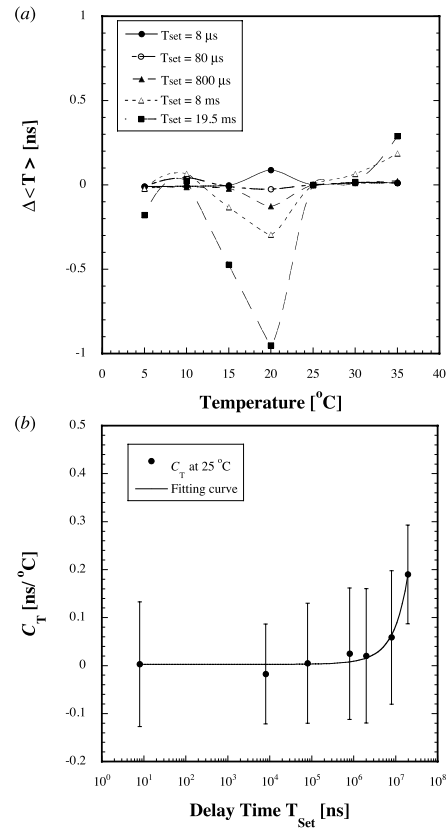


Figure 7: Variations (a) in the difference between the measured time duration and the set delay as a function of temperature, and (b) in the differential coefficient with temperature as a function of the set delay time. The lines indicate a guide for the eyes only in (a) and a second-order polynomial fit to the experimental data in (b).

ternal clock with an accuracy of 0.13 ppm. The results are fully sufficient for monitoring the trigger timing distribution system of the injector linac. The developed TDC could be applied to further complex timing systems in large accelerator complexes.

REFERENCES

- [1] A. Balla *et al.*, Nucl. Instr. and Meth. A 739 (2014) 75.
- [2] S. Kishimoto *et al.*, Nucl. Instr. and Meth. A 731 (2013) 53.
- [3] M. Akemoto *et al.*, Prog. Theor. Exp. Phys. (2013) 03A002.
- [4] K. Furukawa *et al.*, ICALEPCS'13, San Francisco, CA, USA, 2013, pp. 1497 – 1500.
- [5] K. Furukawa *et al.*, PAC'09, Vancouver, British Columbia, Canada, 2009, pp. 4797 – 4799.
- [6] T. Suwada *et al.*, Nucl. Instr. and Meth. A 786 (2014) 83.
- [7] Xilinx Inc., <http://www.xilinx.com/>.
- [8] J. Kalisz, Metrologia 41 (2014) 17.
- [9] SEIKO EPSON Corp., <http://www.epson.com/>.
- [10] L. Zaworski *et al.*, Metrol. Meas. XIX (2012) 115.